in Proc. IST Mobile & Wireless Comm. Summit 2003,
Aveiro (Portugal), June. 2003,
pp. 256–260.

Bit Error Rate Estimation for a Joint Detection Receiver in the Downlink of UMTS/TDD

K. Kopsa, G. Matz, H. Artés, and F. Hlawatsch

Institute of Communications and Radio-Frequency Engineering, Vienna University of Technology
Gusshausstrasse 25/389, A-1040 Wien, Austria
phone: +43 1 58801 38983, fax: +43 1 58801 38999, email: Klaus.Kopsa@nt.tuwien.ac.at

ABSTRACT

The bit error rate (BER) is an important measure of radio link quality in wireless communication systems. In this paper, we show how the BER of a joint detection receiver in the downlink of a UMTS/TDD system can be estimated without an active connection to a base station. We propose estimators for the instantaneous and average uncoded BER that are based on knowledge of the impulse responses and the power levels of surrounding base stations. The accuracy of our BER estimators is assessed through simulation of a UMTS/TDD network with different load factors.

I. INTRODUCTION

Successful operation of third generation networks for mobile communications requires the operator to guarantee a sufficient level of bit error rate (BER) throughout the network. Measuring the BER by means of a trace mobile presupposes an active connection during the whole measurement period, and thus overhead traffic is generated.

In this paper, inspired by the approach described in [1], we present methods for estimating both the instantaneous and the average uncoded BER of a zero forcing (ZF) or minimum mean square error (MMSE) joint detector in the downlink of UMTS/TDD. Our BER estimator does not presuppose an active connection; it only requires knowledge of the power levels and channel impulse responses of surrounding base stations. This knowledge is provided by a network monitoring tool like the one developed within the IST project ANTIUM (see http://www.pcrd-antium.com).

The paper is organised as follows. After a review of some relevant aspects of the UMTS/TDD standard and the development of a signal model in Section II, we derive closed-form expressions for the signal-to-noise-and-interference ratio (SINR) of ZF and MMSE joint detection in Section III. In Section IV, these SINR expressions are used to develop estimators for the instantaneous BER (valid for a single UMTS/TDD timeslot) and for the average BER. Finally, in Section V, the performance of the proposed BER estimation schemes is assessed for a UMTS/TDD system with two different load factors.

Funding by the European IST project ANTIUM and by FWF grant P15156.

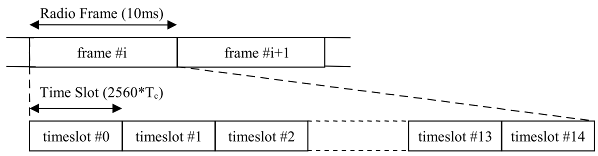

Fig. 1. *Physical channel frame structure* [2].

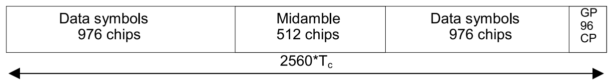

Fig. 2. *Timeslot structure* [2].

II. SIGNAL MODEL

In a UMTS/TDD system, each radio frame consists of 15 timeslots as depicted in Fig. 1 [2]. Each timeslot can be allocated for uplink or downlink in a flexible manner. As shown in Fig. 2, the timeslots consist of two data parts separated by a midamble (which is used for channel estimation) and followed by a guard period. The data parts contain up to 16 data channels. Each data channel uses QPSK modulation and spreading with a different spreading code of length $N = 16$ [3]. Prior to transmission, the sum of the spread data channels is multiplied by a cell-specific scrambling code. Since the scrambling codes in UMTS/TDD also have length 16, we can consider the product of spreading code and scrambling code as one effective spreading code and thus do not have to distinguish between scrambling and spreading. Finally, the signal corresponding to the spread/scrambled data stream is transmitted over a frequency-selective fading channel and received at the mobile receiver.

Let $K_m \leq 16$ denote the number of parallel data streams transmitted by the mth base station to the K_m users active in one particular timeslot (thus, each data stream is associated to an active user). We neglect intersymbol interference (ISI), i.e., our analysis considers only one symbol per user. (This idealisation is well justified because the block processing performed by the receiver effectively removes ISI, cf. Section V.) The K_m QPSK symbols that are transmitted to the

K_m active users can be combined into the $K_m \times 1$ vector

$$\mathbf{s}_m \triangleq [s_{m,1} \cdots s_{m,K_m}]^T .$$

Since the data symbols of different data streams are statistically independent, the correlation matrix of $\mathbf{s}_m$ is given as

$$\mathbf{R}_{\mathbf{s}_m} \triangleq \mathrm{E}\{\mathbf{s}_m \mathbf{s}_m^H\} = \mathbf{A}_m^2 ,$$

where the $K_m \times K_m$ diagonal matrix

$$\mathbf{A}_m \triangleq \mathrm{diag}\{a_{m,1}, \ldots, a_{m,K_m}\}$$

contains the transmit amplitudes of the various data streams that are generally different due to power control.

The effective spreading can be described by the relation

$$\mathbf{d}_m = \sum_{k=1}^{K_m} s_{m,k} \mathbf{c}_{m,k} = \mathbf{C}_m \mathbf{s}_m ,$$

where the $N \times K_m$ code matrix $\mathbf{C}_m$ contains the products of the spreading and scrambling codes of the K_m active users as its columns $\mathbf{c}_{m,k}$. Thus, the $N \times 1$ vector $\mathbf{d}_m$ contains all the chips belonging to the K_m symbols transmitted.

A mobile station located in the first cell[1] (i.e., $m = 1$) receives the signal $\mathbf{d}_1$ from the base station of that cell through an L-tap multipath fading channel with impulse response vector

$$\mathbf{h}_1 \triangleq [h_{1,0} \cdots h_{1,L-1}]^T . \tag{1}$$

The resulting signal component is corrupted by intercell interference from the other $M-1$ base stations, i.e., $\mathbf{d}_m$ for $m = 2, \ldots, M$, and by additive white Gaussian noise. The total received signal is thus given by

$$\mathbf{x} = \mathbf{H}_1 \mathbf{d}_1 + \sum_{m=2}^{M} \mathbf{H}_m \mathbf{d}_m + \mathbf{n} , \tag{2}$$

where $\mathbf{H}_m$, the channel matrix corresponding to the mth base station, is an $(N+L-1) \times N$ Toeplitz matrix given by

$$\mathbf{H}_m \triangleq \begin{bmatrix} h_{m,0} & & \mathbf{0} \\ h_{m,1} & \ddots & \\ \vdots & & h_{m,0} \\ h_{m,L-1} & & h_{m,1} \\ & \ddots & \vdots \\ \mathbf{0} & & h_{m,L-1} \end{bmatrix} ,$$

and $\mathbf{n}$ is a noise vector. Note that $\mathbf{x}$ contains all the chips belonging to the symbol $s_{1,1}$ of interest; furthermore, L is the maximum of the lengths of all channels.

III. SINR CALCULATION

We next consider a linear joint detection receiver that detects the symbols of the K_1 users of the first cell. The received vector $\mathbf{x}$ is passed through an $K_1 \times (N+L-1)$ matrix filter $\mathbf{G}$ that performs channel equalisation and despreading jointly for all users of the first base station. The resulting $K_1 \times 1$ vector

$$\hat{\mathbf{s}}_1 = \mathbf{G}\mathbf{x} = \mathbf{G}\left[\mathbf{H}_1 \mathbf{C}_1 \mathbf{s}_1 + \sum_{m=2}^{M} \mathbf{H}_m \mathbf{C}_m \mathbf{s}_m + \mathbf{n}\right] \tag{3}$$

is an estimate of the weighted symbol vector $\mathbf{s}_1$; it is fed into a decision device to reconstruct the user data. Regarding the choice of $\mathbf{G}$, we will consider the ZF and MMSE joint detectors in what follows [4].

A. ZF Joint Detection

For the ZF joint detector, $\mathbf{G}$ is chosen as the pseudo inverse of the product $\mathbf{H}_1 \mathbf{C}_1$ of channel matrix and code matrix [4, 5]:

$$\mathbf{G} = (\mathbf{C}_1^H \mathbf{H}_1^H \mathbf{H}_1 \mathbf{C}_1)^{-1} \mathbf{C}_1^H \mathbf{H}_1^H .$$

Insertion into (3) gives

$$\hat{\mathbf{s}}_1 = \mathbf{s}_1 + \mathbf{G} \sum_{m=2}^{M} \mathbf{H}_m \mathbf{C}_m \mathbf{s}_m + \mathbf{G}\mathbf{n} .$$

For the first user, this yields

$$\hat{s} = s + e ,$$

where s (which is short for $s_{1,1}$) denotes the symbol of the first user of the first base station, and

$$e = \mathbf{g}^H \sum_{m=2}^{M} \mathbf{H}_m \mathbf{C}_m \mathbf{s}_m + \mathbf{g}^H \mathbf{n} , \tag{4}$$

with $\mathbf{g}^H$ denoting the first row of $\mathbf{G}$, is the intercell interference plus the noise enhanced by $\mathbf{g}^H$. The signals of the other users of the first base station (intracell interference) do not appear in (4) because their influence is completely removed by the ZF filter. Desired signal s and interference/noise e are uncorrelated. The mean power of s is

$$\mathrm{E}\{|s|^2\} = a^2 ,$$

where a is short for the amplitude $a_{1,1}$.

We will next calculate the mean power of e. The code matrix $\mathbf{C}_1$ is known. The channels $\mathbf{H}_m$ are also assumed to be known; this will lead to the derivation of an instantaneous SINR that is valid during a time interval where the channel stays constant (typically one timeslot). Furthermore, because of the properties of the scrambling codes, the columns of the code matrices $\mathbf{C}_m$ of base stations $m = 2, \ldots, M$ can be assumed to be zero-mean, i.i.d. random vectors. Finally, the data symbols of different data streams are statistically independent, and since data symbols, scrambling codes, and noise are also mutually statistically independent, we obtain

$$\begin{aligned} &\mathrm{E}\{|e|^2\} \\ &= \mathrm{E}\left\{\mathbf{g}^H \left(\sum_{m=2}^{M} \mathbf{H}_m \mathbf{C}_m \mathbf{s}_m\right) \left(\sum_{m=2}^{M} \mathbf{s}_m^H \mathbf{C}_m^H \mathbf{H}_m^H\right) \mathbf{g} + \mathbf{g}^H \mathbf{n}\mathbf{n}^H \mathbf{g}\right\} \\ &= \mathbf{g}^H \left(\sum_{m=2}^{M} \mathbf{H}_m \, \mathrm{E}\{\mathbf{C}_m \mathbf{s}_m \mathbf{s}_m^H \mathbf{C}_m^H\} \mathbf{H}_m^H\right) \mathbf{g} + \mathbf{g}^H \, \mathrm{E}\{\mathbf{n}\mathbf{n}^H\} \, \mathbf{g} . \end{aligned}$$

[1] Without loss of generality, we consider BER estimation for the first user of the first base station.

With $\mathrm{E}\{\mathbf{C}_m\mathbf{s}_m\mathbf{s}_m^H\mathbf{C}_m^H\} = \mathrm{E}\{\mathbf{C}_m\mathbf{A}_m^2\mathbf{C}_m^H\} = \eta_m^2\mathbf{I}$ where $\eta_m^2 \triangleq \sum_{k=1}^{K_m} a_{m,k}^2$ and with $\mathrm{E}\{\mathbf{n}\mathbf{n}^H\} = \sigma^2\mathbf{I}$, this becomes

$$\mathrm{E}\{|e|^2\} = \sum_{m=2}^{M} \eta_m^2 \,\|\mathbf{g}^H\mathbf{H}_m\|^2 + \sigma^2\|\mathbf{g}\|^2.$$

Thus, the instantaneous SINR of the ZF joint detector is finally obtained as

$$\gamma \triangleq \frac{\mathrm{E}\{|s|^2\}}{\mathrm{E}\{|e|^2\}} = \frac{a^2}{\sum_{m=2}^{M}\eta_m^2\|\mathbf{g}^H\mathbf{H}_m\|^2 + \sigma^2\|\mathbf{g}\|^2}\,. \tag{5}$$

B. MMSE Joint Detection

The MMSE joint detector does not completely cancel the influence of intracell interference, which results in reduced noise enhancement. Let us rewrite the model (2) as

$$\mathbf{x} = \mathbf{H}_1\mathbf{C}_1\mathbf{s}_1 + \mathbf{w},$$

where $\mathbf{w} \triangleq \sum_{m=2}^{M}\mathbf{H}_m\mathbf{C}_m\mathbf{s}_m + \mathbf{n}$ summarises the signals from base stations other than the first base station and the noise. Note that for the design of the MMSE detector, the channels $\mathbf{H}_m$ ($m = 2,\ldots,M$) are unknown; they will be modeled as random. The MMSE matrix filter $\mathbf{G}$ is now given as [4, 6]

$$\mathbf{G} = \left(\mathbf{R}_{\mathbf{s}_1}^{-1} + \mathbf{C}_1^H\mathbf{H}_1^H\mathbf{R}_{\mathbf{w}}^{-1}\mathbf{H}_1\mathbf{C}_1\right)^{-1}\mathbf{C}_1^H\mathbf{H}_1^H\mathbf{R}_{\mathbf{w}}^{-1}, \tag{6}$$

where $\mathbf{R}_{\mathbf{s}_1}^{-1} = \mathbf{A}_1^{-2}$ and

$$\mathbf{R}_{\mathbf{w}} \triangleq \mathrm{E}\{\mathbf{w}\mathbf{w}^H\} = \mathrm{E}\left\{\sum_{m=2}^{M}\mathbf{H}_m\mathbf{C}_m\mathbf{s}_m\mathbf{s}_m^H\mathbf{C}_m^H\mathbf{H}_m^H\right\} + \mathrm{E}\{\mathbf{n}\mathbf{n}^H\}$$
$$= \sum_{m=2}^{M}\eta_m^2\,\mathrm{E}\{\mathbf{H}_m\mathbf{H}_m^H\} + \sigma^2\mathbf{I}.$$

Under the assumption of uncorrelated scattering and with $L \ll N$, we have

$$\mathrm{E}\{\mathbf{H}_m\mathbf{H}_m^H\} \approx p_m\mathbf{I} \qquad \text{with} \quad p_m \triangleq \sum_{l=0}^{L-1}\mathrm{E}\{|h_{m,l}|^2\},$$

and thus $\mathbf{R}_{\mathbf{w}}$ can be approximated as

$$\mathbf{R}_{\mathbf{w}} \approx \tilde{\sigma}^2\mathbf{I} \qquad \text{with} \quad \tilde{\sigma}^2 \triangleq \sum_{m=2}^{M}\eta_m^2 p_m + \sigma^2. \tag{7}$$

Insertion of (7) into (6) yields after some manipulations

$$\mathbf{G} = \left(\tilde{\sigma}^2\mathbf{A}_1^{-2} + \mathbf{C}_1^H\mathbf{H}_1^H\mathbf{H}_1\mathbf{C}_1\right)^{-1}\mathbf{C}_1^H\mathbf{H}_1^H.$$

Inserting this into (3), we obtain the symbol estimate for the first user as

$$\hat{s} = \mathbf{g}^H\mathbf{H}_1\mathbf{c}_1 s + e,$$

with the interference-plus-noise component

$$e = \mathbf{g}^H\mathbf{H}_1\tilde{\mathbf{C}}_1\tilde{\mathbf{s}}_1 + \mathbf{g}^H\sum_{m=2}^{M}\mathbf{H}_m\mathbf{C}_m\mathbf{s}_m + \mathbf{g}^H\mathbf{n}. \tag{8}$$

Here, $\mathbf{g}^H$ denotes the first row of $\mathbf{G}$, $\mathbf{c}_1$ denotes the first column of $\mathbf{C}_1$, $\tilde{\mathbf{C}}_1$ denotes the matrix $\mathbf{C}_1$ without its first column, and the $(K_1-1)\times 1$ vector $\tilde{\mathbf{s}}_1$ denotes the symbol vector $\mathbf{s}_1$ without the symbol s corresponding to the first user. On the right-hand side of (8), the first term describes residual intracell interference (note that such a term is not present in the corresponding ZF result (4)), the second term describes intercell interference, and the third term represents the enhanced noise component.

The mean power of the desired component $\mathbf{g}^H\mathbf{H}_1\mathbf{c}_1 s$ is

$$\mathrm{E}\{|\mathbf{g}^H\mathbf{H}_1\mathbf{c}_1 s|^2\} = a^2|\mathbf{g}^H\mathbf{H}_1\mathbf{c}_1|^2.$$

The mean power of the interference-plus-noise component e can be calculated as

$$\mathrm{E}\{|e|^2\} = \|\mathbf{g}^H\mathbf{H}_1\tilde{\mathbf{C}}_1\tilde{\mathbf{A}}_1\|^2 + \sum_{m=2}^{M}\eta_m^2\|\mathbf{g}^H\mathbf{H}_m\|^2 + \sigma^2\|\mathbf{g}\|^2,$$

where $\tilde{\mathbf{A}}_1 \triangleq \mathrm{diag}\{a_{1,2},\ldots,a_{1,K_1}\}$ is $\mathbf{A}_1$ with the first row and column removed (note that $\mathrm{E}\{\tilde{\mathbf{s}}_1\tilde{\mathbf{s}}_1^H\} = \tilde{\mathbf{A}}_1^2$). The instantaneous SINR of the MMSE joint detector thus follows as

$$\gamma = \frac{a^2|\mathbf{g}^H\mathbf{H}_1\mathbf{c}_1|^2}{\|\mathbf{g}^H\mathbf{H}_1\tilde{\mathbf{C}}_1\tilde{\mathbf{A}}_1\|^2 + \sum_{m=2}^{M}\eta_m^2\|\mathbf{g}^H\mathbf{H}_m\|^2 + \sigma^2\|\mathbf{g}\|^2}\,. \tag{9}$$

IV. THE BER ESTIMATORS

The interference in (4) and (8) is not Gaussian but it can be approximated by a Gaussian random variable with the same variance as that of the original (non-Gaussian) random variable [4]. Then an estimate for the uncoded instantaneous BER is given by the well-known formula for QPSK modulation with Gray mapping [7]

$$\widehat{\mathrm{BER}} = f(\gamma) = \mathrm{Q}(\sqrt{\gamma}), \tag{10}$$

where γ is the instantaneous SINR as given by (5) or (9) and

$$\mathrm{Q}(x) \triangleq \frac{1}{\sqrt{2\pi}}\int_x^\infty \mathrm{e}^{-t^2/2}\,dt\,.$$

Here, $\widehat{\mathrm{BER}}$ is the BER estimate for a particular channel realisation because the instantaneous SINR γ depends on the M channel matrices $\mathbf{H}_m$ (cf. (5) and (9)).

To obtain an estimate of the uncoded *average* bit error rate $\overline{\mathrm{BER}} \triangleq \mathrm{E}\{\mathrm{BER}\}$, we would have to calculate the average of $\widehat{\mathrm{BER}} = f(\gamma)$ with respect to γ,

$$\mathrm{E}\{f(\gamma)\} = \int_0^\infty f(\gamma)\,p(\gamma)\,d\gamma, \tag{11}$$

where $p(\gamma)$ is the probability density function of γ. Because of the nonlinear dependence of the SINR γ on the channel realisations, $p(\gamma)$ is difficult to compute and the integral (11) cannot be calculated in closed form. Therefore, we will approximate $f(\gamma)$ by a Taylor series about the mean SINR $\bar{\gamma}$ that is truncated after the quadratic term [8]:

$$f(\gamma) \approx f(\bar{\gamma}) + (\gamma-\bar{\gamma})\, f'(\bar{\gamma}) + \frac{(\gamma-\bar{\gamma})^2}{2}\, f''(\bar{\gamma})\,. \qquad (12)$$

Taking the expectation now is easy because it can be done for each term separately and only the mean and variance of γ are required instead of $p(\gamma)$. Using $f(\gamma) = \mathrm{Q}(\sqrt{\gamma})$, we finally obtain

$$\overline{\mathrm{BER}} \approx \mathrm{Q}\big(\sqrt{\bar{\gamma}}\big) + \frac{\mathrm{var}\{\gamma\}}{8\sqrt{2\pi\bar{\gamma}}}\left(1+\frac{1}{\bar{\gamma}}\right) \mathrm{e}^{-\bar{\gamma}/2} \qquad (13)$$

(note that the first-order term in (12) vanished as a result of the expectation operation). In general, the approximation in (12) and, thus, the corresponding approximation in (13) will be accurate if the instantaneous SINR is well concentrated about its mean (i.e., if $\mathrm{var}\{\gamma\}$ is small).

Finally, an estimator $\widehat{\overline{\mathrm{BER}}}$ of the average BER is obtained from the right-hand side of (13) by replacing $\bar{\gamma}$ and $\mathrm{var}\{\gamma\}$ with the sample mean and sample variance of γ, respectively. The sample mean and sample variance are calculated from several measurements of the channels $\mathbf{H}_m$.

V. SIMULATION RESULTS

We will now assess the performance of our BER estimators (10) and (13) through numerical simulations.

A. Simulation Setup

We considered an indoor scenario for UMTS/TDD where the receiver is located within the inner cell of a grid of 8 hexagonal cells with a cell radius of 30 m (see Fig. 3). To vary the SINR, we changed the interference level by loading the network with 2 or 8 users per base station; these users have an equal transmit power of 13 dBm. Furthermore, we varied the background noise power from −30 dBm to −80 dBm and simulated 200 timeslots with different channel realisations for every noise power level.

We used Clarke's channel model [9] according to which the channel weight vector associated to the mth base station and the lth path ($l = 0,\ldots,L-1$; cf. (1)) is given as

$$h_{m,l} = \sum_{p=1}^{N_l^{(m)}} c_{l,p}^{(m)}\, \mathrm{e}^{\mathrm{j}\varphi_{l,p}^{(m)}}\,.$$

Here, $N_l^{(m)}$ is the number of subpaths associated to the lth propagation path, and $c_{l,p}^{(m)}$ and $\varphi_{l,p}^{(m)}$ are respectively the amplitude factor and phase of the pth subpath of the lth path. The phase $\varphi_{l,p}^{(m)}$ was randomly chosen such that a Rayleigh fading channel was obtained. The number of paths (filter taps) was chosen as $L = 3$.

At the receiver, in order to cancel (for the ZF joint detector) or reduce (for the MMSE joint detector) the ISI caused by the multipath fading channel, we stacked the received signal corresponding to a whole timeslot into a vector $\mathbf{x}_{\mathrm{tot}}$ and used an accordingly large matrix filter $\mathbf{G}_{\mathrm{tot}}$. We assumed the channel to be constant during the duration of a UMTS/TDD timeslot (66.7 μs) and only changed the channel realisation from slot to slot. In practice, the loss in BER estimation accuracy caused by the channel's time variation within one timeslot will be small as long as the mobile does not move too fast.

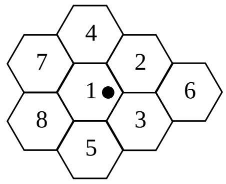

Fig. 3. *Simulation scenario. The bullet • indicates the receiver position.*

B. Results of Instantaneous BER Estimation

Fig. 4 shows the performance of the instantaneous BER estimator (10) for the ZF and MMSE joint detector, respectively. We used UMTS/TDD systems with two users per cell. The circles indicate the measured BER obtained for different SINR values, while the solid line represents the estimated BER as a function of the SINR. (The discrete BER values observed for high SINR are due to the fact that the simulated instantaneous BER is a multiple of 1/244 since one timeslot consists of 244 bits.)

In the low SINR region, the estimation results are seen to be very accurate for both detectors. However, the results are less accurate above an SINR of about 5 dB. An explanation could be that our Gaussian approximation for the total interference becomes less accurate for decreasing noise levels, i.e., when the noise power is well below the power of the co-channel interference. Similar results are obtained for higher load (8 users per cell, not shown here).

C. Results of Average BER Estimation

Fig. 5 shows the estimated average BER (obtained with the estimator (13)) and the measured (simulated) average BER vs. the average SINR for UMTS/TDD systems with 2 and 8 users per cell. The simulated average BER was determined by averaging over 200 instantaneous BER values for each noise power level.

With small load (2 users per cell), the performance of the average BER estimator is seen to be very good for both the ZF and the MMSE joint detector. The estimated and simulated average BER are quite similar all the way from low SINR, where noise is the dominant source of error, to high SINR regions where the noise power is well below the power of the co-channel interference.

In the case of a higher load, we see that our average BER estimator performs well for low SINR. However, its accuracy decreases significantly with increasing SINR, which may be due to the Gaussian interference approximation and/or the truncated Taylor series approximation (12). It is interesting to observe that this effect did not occur in the case of low load.

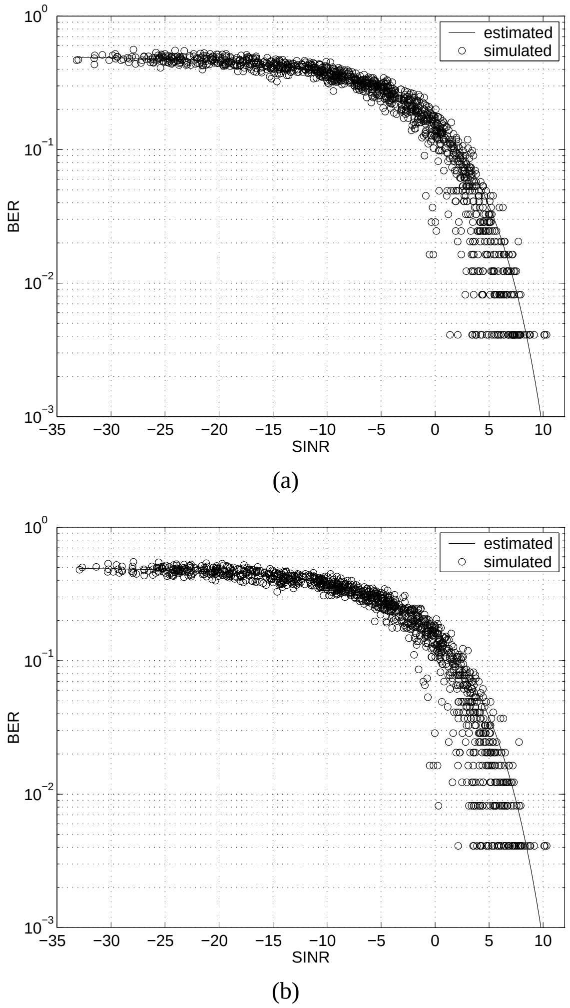

Fig. 4. *Estimated and simulated instantaneous BER for a UMTS/TDD system with load 2: (a) ZF joint detection, (b) MMSE joint detection.*

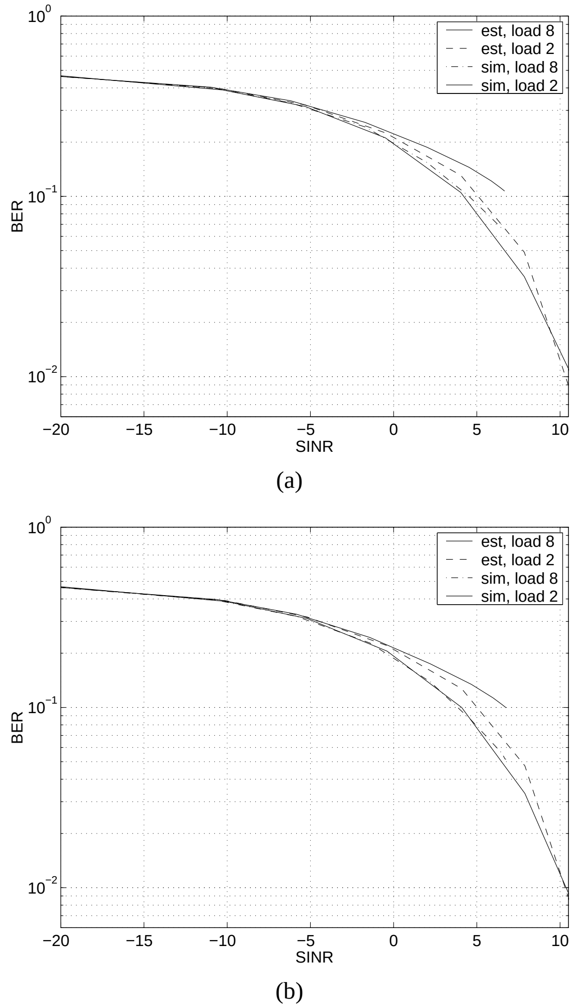

Fig. 5. *Estimated and simulated average BER vs. average SINR for UMTS/TDD systems with load 2 and 8: (a) ZF joint detection, (b) MMSE joint detection. For load 8, the strong co-channel interference causes the SINR to be below about* 6 *dB. (The order of the linetypes in the legend corresponds to the order used in the plot.)*

VI. CONCLUSION

We presented methods for estimating the instantaneous and average uncoded BER of ZF and MMSE joint detection receivers. The proposed BER estimators do not presuppose an active connection to a base station and only require knowledge of the power levels and channel impulse responses of surrounding base stations. An estimator for the instantaneous BER during a particular timeslot was developed using a Gaussian approximation for the co-channel interference and closed-form expressions of the instantaneous SINR. Subsequently, an estimator for the average BER was derived from the instantaneous BER estimator by means of a truncated Taylor series approximation. Simulation results for a UMTS/TDD network with different load factors showed that the proposed average BER estimator is quite accurate except for high SINR when the load is high.

ACKNOWLEDGMENTS

The authors would like to thank P. Loubaton and J.-M. Chaufray for illuminating discussions and helpful suggestions.

REFERENCES

[1] J.-M. Chaufray, W. Hachem, and P. Loubaton, "Asymptotic analysis of optimum and sub-optimum CDMA downlink MMSE receivers," in *Proc. ISIT 2002*, Lausanne, June/July 2002.

[2] 3GPP, "TS 25.221 Physical channels and mapping of transport channels onto physical channels (TDD)," www.3gpp.org, TS 25.221 v. 4.0.0, March 2001.

[3] 3GPP, "TS 25.223 Spreading and modulation (TDD)," www.3gpp.org, TS 25.223 v. 4.0.0, March 2001.

[4] S. Verdú, *Multiuser Detection*, Cambridge Univ. Press, Cambridge (UK), 1998.

[5] L. L. Scharf, *Statistical Signal Processing*, Addison Wesley, Reading (MA), 1991.

[6] C. W. Therrien, *Discrete Random Signals and Statistical Signal Processing*, Prentice Hall, Englewood Cliffs (NJ), 1992.

[7] J. G. Proakis, *Digital Communications*, McGraw-Hill, New York, 3rd edition, 1995.

[8] A. Papoulis, *Probability, Random Variables, and Stochastic Processes*, McGraw-Hill, New York, 3rd edition, 1991.

[9] R. H. Clarke, "A statistical theory of radiomobile reception," *Bell Syst. Tech. J.*, vol. 47, pp. 957–1000, 1968.